The Sensitivity of Tropical Squall Lines (GATE and TOGA COARE) to Surface Fluxes: Cloud Resolving Model Simulations

Yansen Wang[1,2], Wei-Kuo Tao[1], Joanne Simpson[1], and Stephen Lang [1,2]

[1]*Laboratory for Atmospheres*
[2]*Science Systems and Applications Inc.*

NASA/Goddard Space Flight Center
Greenbelt, MD 20771

J. of Atmos . Sci.

(February 24, 1999)

Corresponding author address: Dr. Y. Wang, Mesoscale Atmospheric Processes Branch, Code 912, NASA/ GSFC, Greenbelt, MD 20771

Abstract

Two tropical squall lines from TOGA COARE and GATE were simulated using a two-dimensional cloud-resolving model to examine the impact of surface fluxes on tropical squall line development and associated precipitation processes. The important question of how CAPE in clear and cloudy areas is maintained in the tropics is also investigated. Although the cloud structure and precipitation intensity are different between the TOGA COARE and GATE squall line cases, the effects of the surface fluxes on the amount of rainfall and on the cloud development processes are quite similar. The simulated total surface rainfall amount in the runs without surface fluxes is about 67% of the rainfall simulated with surface fluxes.

The area where surface fluxes originated was categorized into clear and cloudy regions according to whether there was cloud in the vertical column. The model results indicated that the surface fluxes from the large clear air environment are the dominant moisture source for tropical squall line development even though the surface fluxes in the cloud region display a large peak. The high-energy air from the boundary layer in the clear area is what feeds the convection while the CAPE is removed by the convection. The surface rainfall was only reduced 8 to 9% percent in the simulations without surface fluxes in the cloudy region. Trajectory and water budget analysis also indicated that most moisture (92%) was from the boundary layer of the clear air environment.

National Aeronautics and Space Administration

NASA Scientific and Technical Document Availability Authorization (DAA)

The DAA approval process applies to all forms of published NASA Scientific and Technical Information (STI), whether disseminated in print or electronically. It is to be initiated by the responsible NASA Project Officer, Technical Monitor, author, or other appropriate NASA official for all presentations, reports, papers, and proceedings that contain NASA STI. Explanations are on the back of this form and are presented in greater detail in NPG 2200.2, "Guidelines for Documentation, Approval, and Dissemination of NASA Scientific and Technical Information."

[X] Original
[ ] Modified

I. DOCUMENT/PROJECT IDENTIFICATION

TITLE	AUTHOR(S)
"The sensitivity of Tropical squall lines (GATE and TOGA COARE) to surface Fluxes: Cloud resolving model simulations"	Yansen Wang, Wei-Kuo Tao, Joanne Simpson, and Stephen Lang

ORIGINATING NASA ORGANIZATION	PERFORMING ORGANIZATION *(If different)*
NASA Goddard Space Flight Center	

CONTRACT/GRANT/INTERAGENCY/PROJECT NUMBER(S)	DOCUMENT NUMBER(S)	DOCUMENT DATE

For presentations, documents, or other STI to be externally published (including through electronic media), enter appropriate information on the intended publication such as name, place, and date of conference, periodical, or journal name, or book title and publisher in the next box. These documents must be routed to the NASA Headquarters or Center Export Control Administrator for approval (see Sections III and VIII).

▶ J. Atmos. Sci.

II. SECURITY CLASSIFICATION

CHECK ONE *(One of the five boxes denoting Security Classification must be checked.)*

[ ] SECRET [ ] SECRET RD [ ] CONFIDENTIAL [ ] CONFIDENTIAL RD [X] UNCLASSIFIED

III. AVAILABILITY CATEGORY

[ ] ITAR [ ] EAR

Export Controlled Document - USML Category /CCL Export Control Classification Number (ECCN) *(Documents marked in this block must have the concurrence/approval of the NASA Headquarters or Center Export Control Administrator (see Section VIII).)*

Confidential Commercial Document *(check appropriate box at left and indicate below the appropriate limitation and expiration)*:

[ ] TRADE SECRET
[ ] SBIR
[ ] COPYRIGHTED

[ ] U.S. Government agencies and U.S. Government agency contractors only
[ ] NASA contractors and U.S. Government only
[ ] U.S. Government agencies only
[ ] NASA personnel and NASA contractors only
[ ] NASA personnel only
[ ] Available only with the approval of issuing office:
[ ] Limited until *(date)*

[X] PUBLICLY AVAILABLE

Publicly available documents must be unclassified, may not be export controlled, may not contain trade secret or confidential commercial data, and should have cleared any applicable patents application process.

IV. DOCUMENT DISCLOSING AN INVENTION

THIS DOCUMENT MAY BE RELEASED ON *(date)*	NASA HQ OR CENTER PATENT OR INTELLECTUAL PROPERTY COUNSEL SIGNATURE	DATE

V. BLANKET RELEASE (OPTIONAL)

[ ] All documents issued under the following contract/grant/project number may be processed as checked in Sections II and III.

[ ] The blanket release authorization granted on *(date)*

[ ] is RESCINDED - Future documents must have individual availability authorizations.

[ ] is MODIFIED - Limitations for all documents processed in the STI system under the blanket release should be changed to conform to blocks as checked in Sections II and III.

VI. AUTHOR/ORIGINATOR VERIFICATION

I HAVE DETERMINED THAT THIS PUBLICATION:

☐ DOES contain export controlled, confidential commercial information, and/or discloses an invention for which a patent has been applied, and the appropriate limitation is checked in Sections III and/or IV.

☐ does NOT contain export controlled, confidential commercial information, nor does it disclose an invention for which a patent has been applied, and may be released as indicated above.

NAME OF AUTHOR/ORIGINATOR	MAIL CODE	SIGNATURE	DATE
Yansen Wang	912	Yansen Wang	3/2/99

VII. PROJECT OFFICER/TECHNICAL MONITOR/DIVISION CHIEF REVIEW

☒ APPROVED FOR DISTRIBUTION AS MARKED ON REVERSE ☐ NOT APPROVED

NAME OF PROJECT OFFICER OR TECH. MONITOR	MAIL CODE	SIGNATURE	DATE
Franco Einaudi	910	Franco Einaudi	3/18/99

VIII. EXPORT CONTROL REVIEW/CONFIRMATION

☒ Public release is approved ☒ Export controlled limitation is not applicable

☐ Export controlled limitation is approved ☐ Export controlled limitation (ITAR/EAR) marked in Section III is assigned to this document:

USML CATEGORY NUMBER	CCL ECCN NUMBER	HQ OR CENTER EXPORT CONTROL ADMINISTRATOR *(as applicable)*	DATE
N/A	N/A	J. R. Hedgpeth, Code 234	3/21/99

IX. PROGRAM OFFICE OR DELEGATED AUTHORITY REVIEW

☒ APPROVED FOR DISTRIBUTION AS MARKED ON REVERSE ☐ NOT APPROVED

NAME OF PROGRAM OFFICE REPRESENTATIVE	MAIL CODE	SIGNATURE	DATE
Vincent V. Salomonson	900	Vincent V. Salomonson	3/24/99

X. DISPOSITION

THIS FORM, WHEN COMPLETED, IS TO BE SENT TO YOUR CENTER PUBLICATIONS OFFICE

INSTRUCTIONS FOR COMPLETING THE NASA SCIENTIFIC AND TECHNICAL DOCUMENT AVAILABILITY AUTHORIZATION (DAA) FORM

Purpose. This DAA form is used to prescribe the availability and distribution of all NASA-generated and NASA-funded documents containing scientific and technical information (including those distributed via electronic media such as the World Wide Web and CD-ROM).

Requirements. The author/originator must provide either a suitable summary description (title, abstract, etc.) or a completed copy of the document with this form. This form is initiated by the document author/originator and that individual is responsible for recommending/determining the availability/distribution of the document. The author/originator completes Sections I through III, and VI. The author/originator is also responsible for obtaining information and signature in Section IV to the extent the document discloses an invention for which patent protection has been applied. Subsequent to completion of these sections, the author/originator forwards the document to the appropriate Project Manager/Technical Monitor/Division Chief for further review and approval in Section VII, including a re-review of the planned availability and distribution. Once this approval is obtained, the DAA is forwarded to the NASA Headquarters or Center Export Administrator for completion of Section VIII. It is then forwarded for completion of Section IX to the cognizant NASA Headquarters Program Office or Delegated Authority, who provides final review and approval for release of the document as marked.

When to Use This Form. Documents containing STI and intended for presentation or publication (including via electronic media) must be approved in accordance with the NASA STI Procedures and Guidelines (NPG 2200.2). Documents that are to be published in the NASA STI Report Series must be coordinated with the appropriate NASA Headquarters or Center Scientific and Technical Information Office in accordance with NPG 2200.2. Note that information on the Report Documentation Page (if attached) is not to be entered on the DAA except for title, document date, and contract number.

How to Use this Form. Specific guidelines for each section of this form are detailed below.

I. Document/Project Identification. Provide the information requested. If the document is classified, provide instead the security classification of the title and abstract. (Classified information must not be entered on this form). Include RTOP numbers on the Contract/Grant/Interagency/Project Number(s) line. Provide information on presentations or externally published documents as applicable.

II. Security Classification. Enter the applicable security classification for the document. Documents, if classified, will be available only to appropriately cleared personnel having a "need to know."

III. Availability Category for Unclassified Documents. Check the appropriate category or categories.

Export Controlled Document. If the document is subject to export restrictions (see NPG 2200.2, paragraph 4.5.3), the appropriate restriction must be checked, either International Traffic in Arms Regulations (ITAR) or Export Administration Regulations (EAR), and the appropriate United States Munitions List (USML) category or Commerce Control List (CCL), Export Control Classification Number (ECCN) must be cited.

Confidential Commercial Documents (Documents containing Trade Secrets, SBIR documents, and/or Copyrighted Information). Check the applicable box (see NPG 2200.2 paragraph 4.5.7). When any of these boxes are checked, also indicate the appropriate limitation and expiration in the list to the right of these restrictions. These limitations refer to the user groups authorized to obtain the document. The limitations apply both to the initial distribution of the documents and the handling of requests for the documents. The limitations will appear on and apply to reproduced copies of the document. Documents limited to NASA personnel should not be made available to onsite contractors. If the Available Only With the Approval of Issuing Office limitation is checked, the NASA Center for AeroSpace Information will provide only bibliographic processing and no initial distribution; CASI will refer all document requests to the issuing office.

Publicly Available Document - Unrestricted Distribution. Check this box if the information in the document may be made available to the general public without restrictions (unrestricted domestic and international distribution). If the document is copyrighted (see paragraph 4.5.7.3 in NPG 2200.2), also check the "Copyrighted" box in this section.

IV. Document Disclosing an Invention. This must be completed when the document contains information that discloses an invention (see NPG 2200.2, paragraph 4.5.9). When this box is checked, an additional appropriate availability category must be checked. Use of this category must be approved by NASA Headquarters or Center Patent Counsel or the Intellectual Property Counsel.

V. Blanket Release (Optional). Complete this optional section whenever subsequent documents produced under the contract, grant, or project are to be given the same distribution and/or availability as described in Sections II and III. More than one contract number or RTOP Number can be entered. This section may also be used to rescind or modify an earlier Blanket Release. All blanket releases must be approved by the Program Office or its designee and concurred with by the Office of Management Systems and Facilities.

VI. Author/Originator Verification. Required for all DAA forms.

VII. Project Officer/Technical Monitor/Division Chief Review. The Project Officer/Technical Monitor/Author or Originator Division Chief or above must sign and date the form. The office code and typed name should be entered.

VIII. Export Control Review/Confirmation. This section is to be completed by the authorized NASA Headquarters or Center Export Control Administrator for all documents.

IX. Program Office or Delegated Authority Review. This section is to be completed by the duly authorized official representing the NASA Headquarters Program Office. Any delegation from NASA Headquarters to a NASA Center in accordance with NPG 2200.2 should be entered here.

X. Disposition. For NASA Center use.

912 March 1, 1999

TO: 910/Chief, Laboratory for Atmospheres

FROM: Mesoscale Atmospheric Processes Branch/912

SUBJECT: Request for Contractor as Lead Authorship on Attached Paper

Dr. Yansen Wang, lead author of the accompaying manuscript "***The sensitivity of tropical squall lines (GATE and TOGA COARE) to surface fluxes: Cloud resolving model simulations,*** to be submitted to *J. Atmos. Scii.*, developed the most of the ideas and necessary software for the associated research and carried out the numerical experiments, analysis and writing to produce the finished mauscript. The research is a key part of the RTOP (Dr. J. Simpson and Tao are the PI and Co-PI) and NASA TRMM (Dr. Tao and Dr. Simpson are the PI and Co-I) research tasks. This work has been done with PI and Branch Head approval and encouragement.

Wei-Kuo Tao

cc: Dr. Robert Adler

1. Introduction

It is well known that sensible heat, latent heat, and momentum fluxes between the ocean and the atmosphere play an important role in cloud development and precipitation processes over the ocean. Surface fluxes are temporally and spatially complex in the region of active convection. For example, earlier observational studies (Malkus and Ronne, 1954; Malkus, 1958; LeMone and Pennell 1976) have demonstrated that formation of oceanic cumulus clouds in the trade winds is controlled largely by marine boundary layer processes. Observational studies in the Western pacific warm pool region (Bradley, 1991; Young *et al.*, 1992; Fairall *et al.*, 1996) have shown that surface heat and momentum fluxes all have a peak in the convective leading edge due to strong gust winds and colder air temperatures in the convective region. The surface fluxes in the large clear area are much smaller and more uniform than those in the convective region. Several numerical modeling studies (Tao *et al.*, 1991; Wang *et al.*, 1996) have indicated that sensible and latent heat fluxes can enhance surface precipitation and cloud coverage by comparing simulations with and without the effects of ocean fluxes for both subtropical (TAMEX) and tropical (TOGA COARE) squall lines. Wang *et al.* (1996) also showed that among the heat and momentum fluxes, the latent heat flux is the most important component for cloud development. However, those studies left following question unanswered, which part of the surface fluxes, those in the large clear air environment or those in the convective area, is responsible for enhancing cloud development and precipitation?

In this sensitivity study, simulations were made for two well documented tropical squall lines, the 12 September 1974 GATE (Szoke and Zipser, 1986) and the 22 February 1993 TOGA COARE cases (Jorgensen *et al.*, 1997). Both cases, TOGA COARE and GATE, (Table 1) have moderate convective available potential energy (CAPE), 1400 and 1600 J/kg, respectively. Tropical oceanic convective systems are typically associated with a moderate CAPE. While the TOGA COARE case has a very moist environment with a precipitable water of 6.05 g cm^{-2} , the GATE case is substantially drier with a precipitable water of 4.80 g cm^{-2}. The sea surface temperature in the TOGA COARE case is higher that that in the GATE case. The surface heat fluxes are strongly dependent on the temperature difference between the air and the sea sureface. The environmental

winds are also quite different between the two cases. In the TOGA COARE case, a fairly strong low level jet (about 12 m s^{-1}) is present at a height of 2 km, and there is a weak overturning upper tropospheric wind (4 ms^{-1}) at about 10 km. The GATE case has less shear in the lower troposphere, but there is a strong jet in the upper troposphere above 10 km (about 30 m s^{-1}) in the same direction as the low level flow.

The objective of this study is to identify which part of the surface fluxes, the clear large-scale environment or the cloudy region with strong gust winds, is more influential in the development and precipitation processes of tropical squall lines. The important question of how CAPE in clear and cloudy areas is maintained in the tropics is also investigated. The two well-documented tropical squall lines cases from GATE and TOGA COARE, that occurred in quite different large scale environments, are simulated and the results are analyzed.

2. Model and Model Setup

The tool used in this study is the two-dimensional version of the Goddard Cumulus Ensemble (GCE) model. The simulated flow is assumed to be anelastically balanced. Sound waves have been filtered out by neglecting the local variation of air density with time in the mass equation. The cloud microphysics include a parameterized Kessler-type two-category liquid water scheme (cloud water and rain), and a parameterized Lin et al. (1983) or Rutledge and Hobbs (1984) three-category ice-phase scheme (cloud ice, snow and hail/graupel). Short-wave (solar) and long-wave (infrared) radiation parameterizations (Chou 1984; 1986) as well as a subgrid-scale turbulence (one-and-a-half order) scheme are also included in the model.

The GCE model has implemented a Multi-dimensional Positive Definite Advection Transport Algorithm (Smolarkiewicz and Grabowski, 1990). All scalar variables (potential temperature, water vapor, turbulence coefficient and all five hydrometeor classes) used forward time differencing and the MPDATA for advection. The dynamic variables, u, v and w, used a second-order accurate advection scheme and a leapfrog time integration (kinetic energy semi-conserving method). A stretched vertical coordinate (height increments from 40 to 1150 m) with 31 grid points was used to maximize resolution in the lowest

levels of the model. A total of 1024 grid points were used in the horizontal with 750 m resolution. Details of the model description can be found in Tao *et al.* (1993), Tao and Simpson (1993), and Simpson and Tao (1993).

The surface flux parameterization used in this study is from the TOGA COARE flux algorithm (Fairall *et al.*, 1996). This is primarily based on the bulk scheme developed by Liu *et al.* (1979), which has shown good agreement with observations (Bradley *et al.*, 1991). The transfer coefficients for momentum, sensible heat, and latent heat fluxes are based on the Monin-Obukhov similarity theory of the atmospheric surface layer (Businger *et al.*, 1971). This bulk scheme has been modified (Fairall *et al.*, 1996) to better simulate surface fluxes from the tropical ocean and calibrated by the large amount of data from the TOGA COARE field experiment.

The shortwave radiation models of Chou (1992) are used to compute solar heating in the atmosphere and clouds and at the surface. The longwave radiation of Chou and Suarez (1994) is used to compute cloud and atmospheric infrared cooling. The cloud optical properties are parameterized using a broadband emissivity method (Stephens, 1984). Both the liquid and solid phase of the water as well as their size distribution are used in the parameterization. Details of the cloud optical calculations and their sensitivity tests, as well as a review of cloud resolving modeling studies on the cloud-radiation interactions can be found in Tao *et al.* (1996).

The soundings used for this sensitivity study are from two well-documented squall line cases, the 22 February 1993 TOGA COARE (Wang et al., 1996) case, and the 12 September 1974 GATE case (Ferrier et al., 1995). The set-up for the model domains and boundary conditions for both cases are the same. The model domain consists of 1024 horizontal and 31 vertical grid points with open lateral boundary conditions. A constant horizontal grid spacing of 0.75 km in the interior 864 grid points is placed within a coarser, horizontally stretched outer region with a stretching ratio of 1.05, resulting in 18506 km of total horizontal model domain with 684 km being constant resolution. The vertical coordinate is stretched in order to maximize resolution in the lowest levels of the domain. The vertical grid spacing increases from 40 m near the surface to 1164 m at the top of the 21.5-km deep domain.

3. Sensitivity test of surface fluxes

The experiments designed to test the influence of surface fluxes on tropical squall lines from different regions is listed in Table 2 (T for TOGA COARE and G for GATE). The control runs (T1 and G1) have all the model physics, including surface fluxes over the whole computational domain. Runs T2 and G2 have no surface fluxes anywhere in the entire simulation domain. The surface fluxes were set to zero in the cloudy region in runs T3 and G3, and the surface fluxes in the clear region were set to zero in the runs T4 and G4. The clear and cloudy regions were determined at every time step using a total hydrometeor content of 10^{-5} g/g as a threshold value. Every column in the domain was searched vertically to determine whether the column was clear or cloudy. If it exceeded the threshold at any level, it was considered cloudy. The largest amount of cloud coverage at any time in any run was about 1.6% (300 km) of the simulation domain including both TOGA COARE and GATE cases.

3.1 Surface precipitation characteristics

Squall line convection can alter the sea surface fluxes in the cloudy area. Fig. 1 shows the instantaneous surface momentum and heat fluxes at 10 hours into the GATE control simulation (G1). Similar flux characteristics for the TOGA COARE case were shown in Wang et al., (1996). The average latent heat flux in the clear area for TOGA COARE (80 wm^{-2}) is greater than that in the GATE case (60 wm-2). This is primarily due to the fact that the TOGA COARE case has a larger air-sea surface temperature difference. Both cases show a large jump in fluxes at the leading edge of the squall line systems due to the strong surface winds. Following the peak, there is a transitional area where the surface fluxes gradually decrease to the values of the environment.

The domain averaged total surface rainfall amounts from the various simulations are listed in Table 3. The TOGA COARE and GATE runs give consistent results: the least rainfall was from the runs without surface fluxes, and the most rainfall was from the control cases. Although the magnitude of the fluxes in the convective region is large due to stronger surface winds, the surface fluxes from the clear area have a much greater influence on the surface rainfall

than the fluxes from the cloudy area. The runs without surface fluxes in the cloudy region have a 5 to 10% rainfall reduction, verses a 26% rainfall reduction in the runs without surface fluxes in the clear region. Time-space plots of surface rainfall every three minutes are shown in Fig 2 and Fig 3 for TOGA COARE and GATE, respectively. The figures indicate that the precipitation patterns in the early stage of the storms are quite similar for all runs in each squall line case. However, the rainfall amounts started to diverge as the squall lines reached their mature stage (about 4 hours). The runs without any surface fluxes and without surface fluxes in the clear area showed a greater decrease in surface precipitation than the run with surface fluxes only in the clear area.

Model simulated rainfall is also separated into stratiform and convective components according to the method proposed by Tao et al. (1993). Table 3 lists the stratiform rainfall amount and percentage of the total rainfall that is strtiform for all the runs. The results from TOGA COARE and GATE are not consistent. The TOGA COARE runs indicate that the surface fluxes increase stratiform rainfall, while the GATE runs do not show this. Instead, the percentage of the stratiform rainfall showed mixed results. This inconsistency was caused by small convective cells in front of the main squall line in the GATE runs (Fig. 3) in which the rainfall is mostly convective. Those secondary convective cells are caused by gravity wave from the main squall line convection which will be discussed in the next section.

3.2 *Cloud structure*

To examine the cloud structure and cloud coverage, hydrometeor contours are plotted for the TOGA COARE runs at 8 hours in Fig. 4 and the GATE runs at 12 hours in Fig.5. Since the maximum updrafts are greater in the GATE case (12 ms-1) than in the TOGA COARE case (8.5 ms-1) at this time (Fig. 6), the TOGA COARE squall line has much shallower convection (4.5 km) compared with the GATE squall line. The cloud coverage response to the surface fluxes is similar for both cases. Fig. 5 shows that cloud coverage is larger for the runs with surface fluxes (control run G1) and with surface fluxes in the clear region (G3) compared to those runs without surface fluxes (G2) and with surface fluxes in the cloudy region only (G4). Cloud coverage in the TOGA COARE case (Fig. 4) is also slightly larger for the runs with surface fluxes (T1) and with surface fluxes in the clear

region (T3). The increase in cloud coverage was caused by the moisture input from the sea surface evaporation in the cases with surface fluxes. Differences in cloud coverage for these various runs are consistent over the whole time period of simulation time.

Although the squall line precipitation amounts responded similarly to the surface fluxes in similar trend, there was a difference in the convective cell generation ahead of the main line system between the TOGA COARE and GATE cases. The GATE case had stronger peak updrafts (Fig. 6) and taller convective cores compared with the TOGA COARE case (see Figs. 4, 5). The TOGA COARE simulations did not produce any convective cells ahead of the main squall system because of the weaker and more uniform updrafts, while the GATE simulations generated several convective cells in front of the main squall line (Fig. 3). These convective cells are generated by gravity waves excited from the convective cores of the squall line. As indicated in Fig. 6, the runs with surface fluxes (G1) or with surface fluxes in the clear area (G3) have greater vertical velocities compared with runs G2 and G4. Therefore the G1 and G3 had more secondary convective cells ahead of the main squall line.

3.3 *Convective Available Potential Energy (CAPE)*

Fig. 7 and Fig. 8 show the space-time variation of the CAPE values in the TOGA COARE runs (T1, T2, T3, T4) and the GATE runs (G1, G2, G3, G4), respectively. The CAPE values were computed from model results at each half hour using GEMPAK (General Meteorological Package, desJardins et al., 1991). First, there are significant differences in the low CAPE (< 100 J/kg) region between the TOGA COARE and GATE runs. The GATE runs show much broader low CAPE bands and wake compared with the TOGA COARE runs. These differences are primarily caused by the more intense convection in the GATE case. Fig.9 shows the averaged profiles of temperature and moisture differences from the initial soundings averaged over the 150-km cloud band. The GATE case shows much greater mid-tropospheric warming and lower tropospheric drying, and therefore larger area of low CAPE after the convection.

The main effects of the surface fluxes on the CAPE values are in the clear region. With environmental surface fluxes turned on in runs T1 and G1 and

runs T3 and G3, the CAPE values show less variation from start to the end compared to runs T2 and G2 and runs T4 and G4. Table 4 show that the CAPE values increase gradually with time from 1418 to 1586 J/kg for run T1, while the CAPE decreases little from 1625 to 1350 for run G1. This discrepancy between TOGA COARE and GATE is probably due to two reasons: the larger air-sea surface temperature difference and hence the larger surface fluxes in the TOGA COARE case and the stronger convergence of the GATE case. The runs without surface fluxes (T2, G2) in the clear region showed the largest decrease in CAPE in the clear region with respect to time due to the lack of moisture supply from the sea surface.

Our analysis indicated that latent heat flux is the dominant source of CAPE compared to sensible heat flux. Four supplementary runs were carried out for this purpose. In the TOGA COARE case, the average value of CAPE in the clear region decreases from 1418 to 812 J/kg over the 16 hour simulation without latent heat flux, while CAPE increased slightly from 1416 to 1504 in a run without sensible heat flux. Similarly in the GATE case, a run without latent heat flux yields a large decrease in CAPE from 1625 to 850 J/kg, while a run without sensible heat flux had a relatively modest decrease in CAPE, from 1600 to 1300 J/kg. This indicated that surface fluxes, especially latent heat fluxes are a major source of CAPE.

It appears that CAPE values in the clear region are closely related to the total amount of surface precipitation in both the TOGA COARE and GATE cases. For example, in runs G1 and G3, the CAPE values are similar (Fig.7), and there is little difference (8%) in surface rainfall between those two runs. However, CAPE values decreased greatly from start to finish in runs G2 and G4, and the rainfall amounts had a greater percentage decrease (26%, see Table 3) as well. Similar conclusions apply to the TOGA COARE case. Since both the TOGA COARE and the GATE squall lines propagated quickly, the CAPE values in the clear regions out ahead of the systems determined the parcel buoyancy and vertical wind speed and therefore the intensity of the convection.

3.4 Trajectory analysis and water budget analysis

As described in the previous sections, the precipitation, the domain averaged CAPE, and the cloud structure, all show remarkable similarity for the simulations with surface fluxes (control) and with surface fluxes in the clear region. This indicated that surface fluxes from the cloudy region had only a secondary influence on cloud development compared with those from the large clear area, even though the surface fluxes in the cloudy region can be almost 5 to 7 times that of the clear area (see Fig 1). The cloudy area is too small to have a significant amount of moisture input. To support this conclusion, further analysis on the simulations has been performed.

Fig. 10 and Fig. 11 show backward trajectories from the TOGA COARE and GATE control runs (T1 and G1). The trajectory analysis used the model-simulated results from every three minutes and the data was linearly interpolated. The primary inflow of moist air is from in front of the squall line, and that air rises through the convective cores of the squall line. Nine parcels from the boundary layer out in front of the main squall line were randomly chosen. The trajectories indicated that cloud parcels mostly originated from the convective leading edge, and parcels from the leading convective edge are mostly from the clear area in front. These parcels ascended rapidly in a narrow convective updraft up to 4 to 6 km before getting transported to the stratiform region of the cloud system.

Moisture enters the squall line convection mainly from two locations: advection of moist boundary layer air from out ahead of the squall line and surface moisture flux from directly beneath the convection. The boundary layer moisture in the clear area comes directly from evaporation of the ocean surface. Sensitivity tests have indicated that moisture flux is the most important factor in sustaining the CAPE. The amount of water vapor flowing into the convection from these two sources can be estimated from the cloud model results and from the surface flux calculations. Water vapor influx from the leading edge was estimated by integrating the horizontal moisture flux up to a 2 km height using the storm-relative U and the corresponding water vapor mixing ratio q in front of the squall line (about 4 km ahead of the convective core, see Fig.12). Table 5 gives average moisture inflow values per unit meter of squall line computed from the three-minute cloud model data for both TOGA COARE and GATE. The moisture flux directly beneath the cloud contributed less than 8% of the total

moisture. These results show why the surface flux in the large clear area has a greater effect on the squall line precipitation. More than 92% of the moisture comes from the boundary layer of the environment, which is ultimately from the surface moisture flux. The above analysis indicates that correct specification of fluxes in the clear region is very important in tropical squall line system modeling.

4. Summary and Conclusions

A two-dimensional cloud-resolving model is linked with a TOGA COARE flux algorithm to examine the impact of ocean surface fluxes on tropical squall line development and its associated precipitation processes. The distribution of CAPE in the model domain was also examined over the course of the cloud development. Although the cloud structure and precipitation intensity are different between the TOGA COARE and GATE squall line cases, the effects of the surface fluxes from different regions on the amount of rainfall and the cloud development processes are quite similar. The simulated total surface rainfall amount in the runs without surface fluxes is about 67% of the rainfall simulated with surface fluxes. The model results also indicate that the surface fluxes from the large clear environment are the dominant moisture source for tropical squall line development. Surface rainfall was reduced 8 to 9% in simulations without surface fluxes in the cloud region. Trajectory and water budget analysis indicated that most moisture (92%) is from the boundary layer of the clear environment air even though moisture fluxes are large in the cloudy region. Tropical squall lines feed on high CAPE air in the front of the convection, and they leave a low CAPE wake behind them. The conclusion is that accurate specification of the surface fluxes in the large environmental area is more critical when simulating air-sea interactions.

In the tropical atmosphere, CAPE is relatively uniform and moderate over wide areas. Comparisons between soundings made in clear areas remote from cumulus clusters with those made in clear spaces within cloud clusters showed a steeper lapse rate in the ones far from cloudy areas (Bunker et al., 1949; Malkus, 1958). Surface energy fluxes from the sea steepen the lapse rate, while transports by cumulus clouds work to restore a most adiabatic lapse rate (Riehl, 1954). Model simulations of tropical squall lines agree with those conclusions. As a

continuation of this study, the 3D version of the GCEmodel will be used to simulate the PBL structure in both the clear and disturbed regions of various type of cloud systems (i.e. , fast/slow-moving squall system, and rotating MCS's) for comparison with COARE observations. Trajectory analysis of both the inflow and the outflow of various cloud systems along with changes in the ambient CAPE will also be documented.

5. Acknowledgments

This work is supported by the NASA Headquarters Physical Climate Program and the NASA Tropical Rainfall Measuring Mission (TRMM). These authors are grateful to Dr. R. Kakar for his support of this research. Acknowledgment is also made to NASA/Goddard Space Flight Center for computer time used in the research.

6. References

Bradley, E. F., P. A. Coppin, and J. S. Godfrey, 1991: Measurements of sensible and latent heat flux in the western tropical Pacific Ocean. *J. Geophys. Res.*, **96**, 3375-3389.

Bunker, A. F., B. Haurwitz, J. S. Malkus, and H Stommel, 1949: Vertical distribution of temperature and humidity over the *Caribbean sea. Pap Phys. Oceang. and Meteoro.*, MIT and Woods Hole Ocean. Inst., II, No. 1, 82pp.

Businger, J. A., J. C. Wyngaard, Y. Izumi, and E.F. Bradley, 1971: Flux profile relationships in the atmospheric surface layer. *J. Atmos. Sci.*, **28**, 181-189.

Chou, M.-D., 1992: A solar radiation model for use in climate studies. *J. Climate.*, **49**, 762-772.

Chou, M.-D., and M. J. Suarez, 1994: An efficient thermal infrared radiation parameterization for use in general circulation models. NASA Tech. Memo. 104606, 85 pp.

Fairall C., E.F. Bradley, D.P. Rogers, J.B. Edson, and G. S. Young, 1996: Bulk parameterization of air-sea fluxes for TOGA COARE. *J. Geophy. Res.*, **101**, 3747-3764.

Ferrier, B. S., W. -K. Tao, and J. Simpson, 1995: A double-moment multiple-phase four-class bulk ice scheme. Part II: Simulations of convective storms in different large-scale environments and comparisons with other bulk parameterizations. *J. Atmos. Sci.*, **52**, 1001-1033.

Jorgensen, D. P., M. A. LeMone, and S. B. Trier, 1997: Structure and evolution of the 22 February 1993 TOGA COARE squall line: Aircraft observations of precipitation, circulation, and surface fluxes. *J. Atmos. Sci* **125**, 1961-1985.

LeMone, M. A. and W. T Pennell, 1976: The relationship of trade wind cumulus distribution to subcloud layer fluxes and structure. *Mon. Wea. Rev*, **104**, 524-539.

Liu, W. T., K. B. Katsaros, and J. A. Businger, 1979: Bulk parameterization of the air-sea exchange of heat and water vapor including the molecular constraints at the interface. *J. Atmos. Sci.*, **36**, 1722-1735.

Lin, Y.-L., R. D. Farley and H. D. Orville, 1983: Bulk parameterization of the snow field in a cloud model. *J. Clim. Appl. Meteor.*, **22**, 1065-1092.

Malkus, J. S. , 1958: On the structure of the trade wind moist layer. *Physical Oceannography and Meteorology,* Massachusetts Institute of Technology and Woods Hole Oceanographic Institute Monogr. No. 2, 47pp.

Malkus, J. S. and C. Ronne, 1954: On the structure of some cumulonimbus clouds which penetrated the high tropical troposphere. *Tellus,* **4,** 351-366.

Riehl, H. , 1954: Variations of energy exchange between sea and air in the trades. *Weather*, **9**, 355-340.

Rutledge, S.A., and P.V. Hobbs, 1984: The mesoscale and microscale structure and organization of clouds and precipitation in midlatitude clouds. Part II: A diagnostic modeling study of precipitation development in narrow cold frontal rainbands. *J. Atmos. Sci.*, **41**, 2949-2972.

Smolarkiewicz, P. K., and W. W. Grabowski, 1990: The multidimensional positive advection transport algorithm: Nonoscillatory option. *J. Comput. Phys.*, **86**, 355-375.

Simpson, J. and W.-K. Tao, 1993: The Goddard Cumulus Ensemble Model. Part II: Applications for studying cloud precipitating processes and for NASA TRMM. *Terrestrial, Atmospheric and Oceanic Sciences*, **4**, 73-116.

Stephens, G. L., 1984: The parameterization of radiation for numerical weather prediction and climate models. *Mon. Wea. Rev.* , **112,** 826-867.

Szoke, E. J. and E. J. Zipser, 1986: A radar study of convective cells in mesoscale systems in GATE. Part II. Life cycles of convective cells. *J. Atmos. Sci.*, **43**, 199-218.

Tao, W.-K., and J. Simpson, 1993: The Goddard Cumulus Ensemble Model. Part I: Model description. *Terrestrial, Atmospheric and Oceanic Sciences*, **4**, 35-72.

Tao, W.-K., J. Simpson and S.-T. Soong, 1991: Numerical simulation of a sub-tropical squall line over Taiwan Strait. *Mon. Wea. Rev.*, **119**, 2699-2723.

Tao, W.-K., J. Simpson, C.-H. Sui, B. Ferrier, S. Lang, J. Scala, M.-D. Chou and K. Pickering, 1993: Heating, moisture and water budgets of tropical and midlatitude squall lines: Comparisons and sensitivity to longwave radiation. *J. Atmos. Sci.*, **50**, 673-690.

Tao W. -K., S. Lang, J. Simpson, C. -H. Sui, B. Ferrier, and M. -D. Chou, 1996, Mechanisms of cloud-radiation interaction in tropics and midlatitudes. J . Atmos. Sci., 53. 2624-2651.

Wang, Y., W.-K. Tao, and J. Simpson, 1996: The impact of ocean surface fluxes on a TOGA COARE convective system. *Mon. Wea. Rev.*, **124**, 2753-2763.

Young, G. S., D. V. Ledvina, and C. W. Fairall, 1992: Influence of precipitating convection on the surface energy budget observed during a tropical ocean global atmosphere pilot cruise in the tropical western pacific ocean. *J. Geophy. Res.*, **97**, 9595-9603.

Table Captions

Table 1 Initial environmental conditions expressed in terms of CAPE, precipitable water, sea surface temperature (SST), surface air temperature, water vapor and wind for the TOGA COARE and GATE squall cases.

Table 2 Setups for the eight sensitivity experiments conducted.

Table 3 Surface rainfall amounts accumulated over 16 hours and normalized against a control run (T1 and G1). The amount as well as the percentage of rainfall that was stratiform are also given.

Table 4 The average CAPE (J/kg) in the clear area at the end of each sensitivity test.

Table 5 Moisture contributions (kg s^{-1} m^{-1}) from the cloudy region and from the leading edge of the squall system.

Figure Captions

Fig. 1 Spatial variation of (a) rain rate, (b) surface frictional velocity, (c) latent heat flux (LH), and (d) sensible heat flux (SH) at 10 hours into the simulation.

Fig. 2 Space-time distribution of surface rain rate (mm/hr) for the TOGA COARE runs (T1, T2, T3, T4).

Fig. 3 Space-time distribution of surface rain rate (mm/hr) for the GATE runs (G1, G2, G3, G4).

Fig. 4 Vertical cross-sections of total hydrometeors at 8 hours into the TOGA COARE simulations (T1, T2, T3, T4).

Fig. 5 Vertical cross-sections of total hydrometeors at 12 hours into the GATE simulations (G1, G2, G3, G4).

Fig. 6 Maximum updrafts (every 3 minutes) in the TOGA COARE (T1, T2, T3, T4) and GATE (G1, G2, G3, G4). The traces were smoothed by a running average of 5 points.

Fig. 7 Space-time plots of the CAPE (J/kg) in the TOGA COARE runs (T1, T2, T3, T4).

Fig. 8 Space-time plots of the CAPE (J/kg) in the GATE runs (G1, G2, G3, G4).

Fig. 9 Average temperature (DT) and moisture differences (DQ) from the initial soundings. The average was taken over the 150 km cloudy areas in runs T1 and G1.

Fig. 10 Backward trajectories from 9 parcels from the TOGA COARE control run (T1).

Fig. 11 Backward trajectories from 9 parcels from the GATE control run (G1).

Fig. 12 Schematic diagram showing the computation of moisture fluxes from in front of the squall line and from the surface beneath the cloudy region.

TABLE 1

	CAPE (J/kg)	Precipitable water (g/ cm^2)	SST (°C), Tsfc (°C) Qsfc (g/kg), Usfc (m/s)
TOGA COARE	1418	6.05	28.0, 26.8 20.01, 3.20
GATE	1625	4.80	26.9, 26.2 17.33, 0.43

TABLE 2

	TOGA COARE	GATE
Surface fluxes + LW + SW radiation (Control run)	T1	G1
No Surface fluxes	T2	G2
No surface fluxes in Cloudy Region	T3	G3
No surface fluxes in Clear region	T4	G4

TABLE 3.

	TOGA COARE				GATE			
Run number	T1	T2	T3	T4	G1	G2	G3	G4
Domain average total rainfall (mm/16hr), Percentage relative to control run	5.27 (100%)	3.53 (67%)	4.84 (92%)	3.78 (74%)	9.36 (100%)	6.30 (67%)	8.48 (91%)	6.97 (74%)
Stratiform rainfall (mm/16hr), Percentage relative to its total	2.48 (47%)	1.27 (36%)	2.27 (47%)	1.40 (37%)	2.71 (29%)	2.33 (37%)	3.13 (37%)	1.81 (26%)

Table 4.

TOGA COARE Initial CAPE: 1418 (J/kg)				GATE Initial CAPE: 1625 (J/kg)			
T1	T2	T3	T4	G1	G2	G3	G4
1586	754	1510	858	1350	810	1302	854

Table 5

	moisture from leading edge of squall line	moisture from cloudy region
GATE	137.6	9.8
TOGA COARE	70.4	6.1

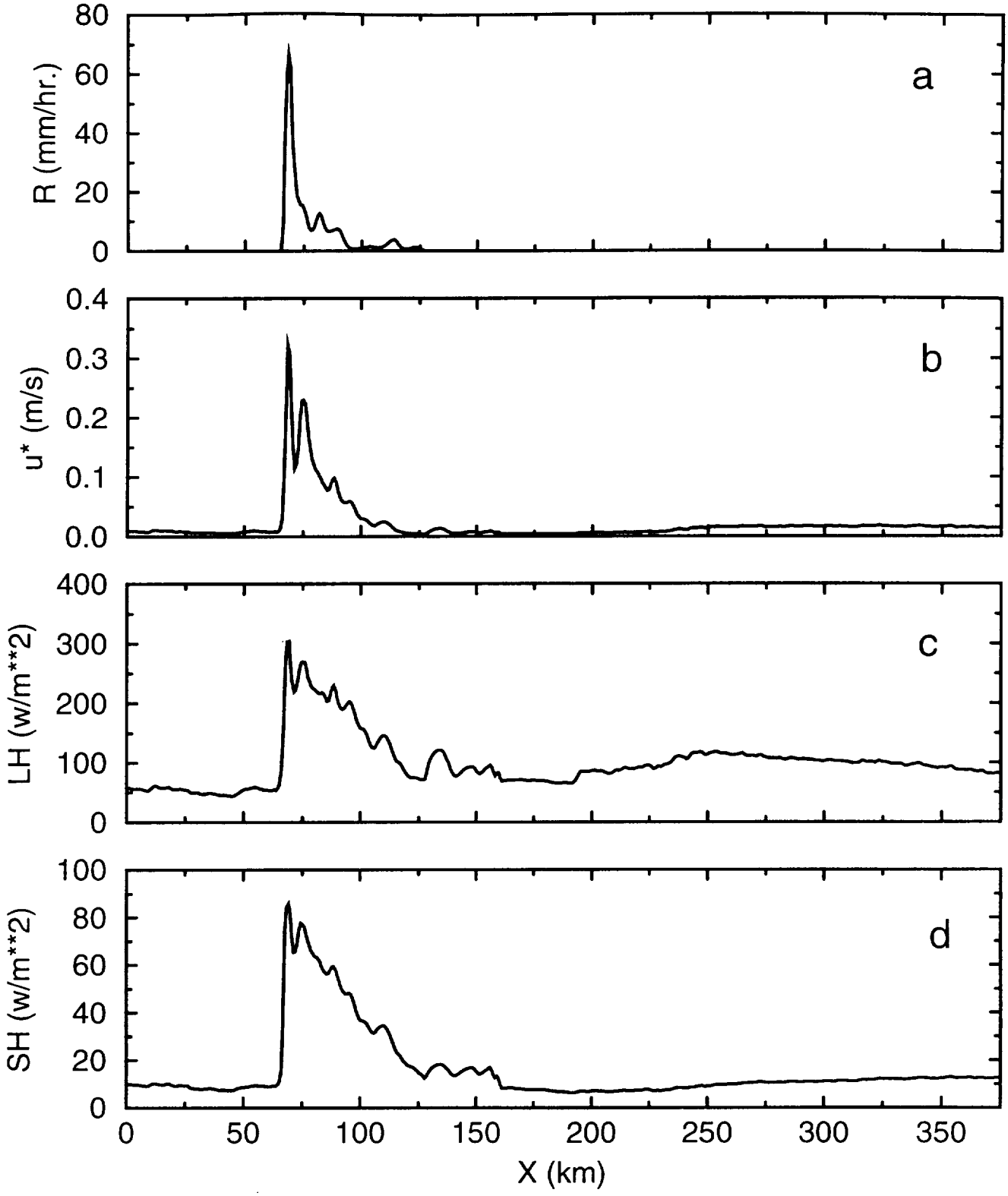
a
b
c
d
R (mm/hr.)
u* (m/s)
LH (w/m**2)
SH (w/m**2)
X (km)
0
20
40
60
80
0.0
0.1
0.2
0.3
0.4
100
200
300
400
50
150
250
350

Fig 1

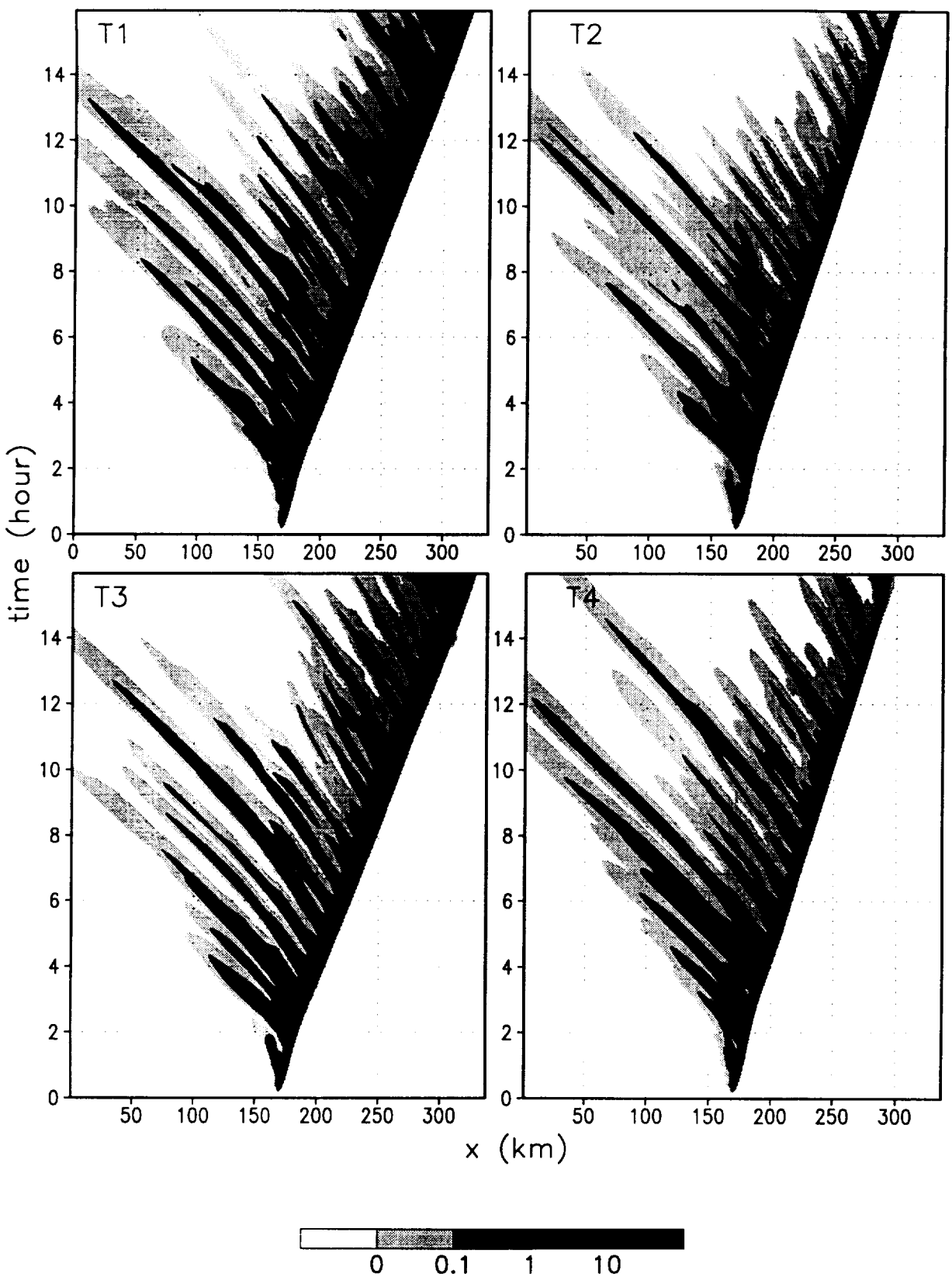
TOGA COARE rainfall distribution (mm/hr)
T1
T2
T3
T4
time (hour)
x (km)
0
50
100
150
200
250
300
2
4
6
8
10
12
14
0
0.1
1
10

Fig. 2

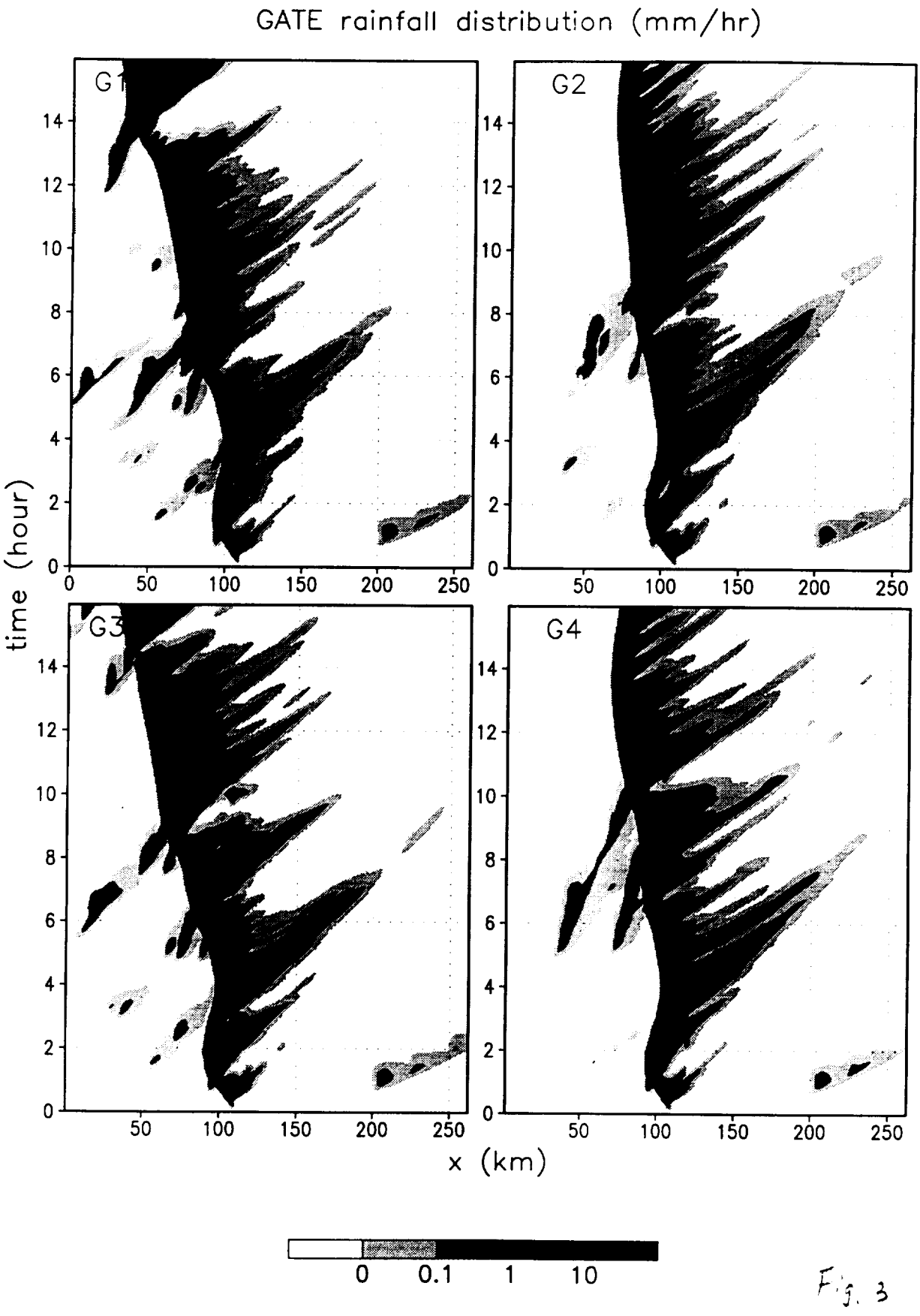
GATE rainfall distribution (mm/hr)
G1
G2
G3
G4
time (hour)
x (km)
0
50
100
150
200
250
2
4
6
8
10
12
14
0
0.1
1
10

Fig. 3

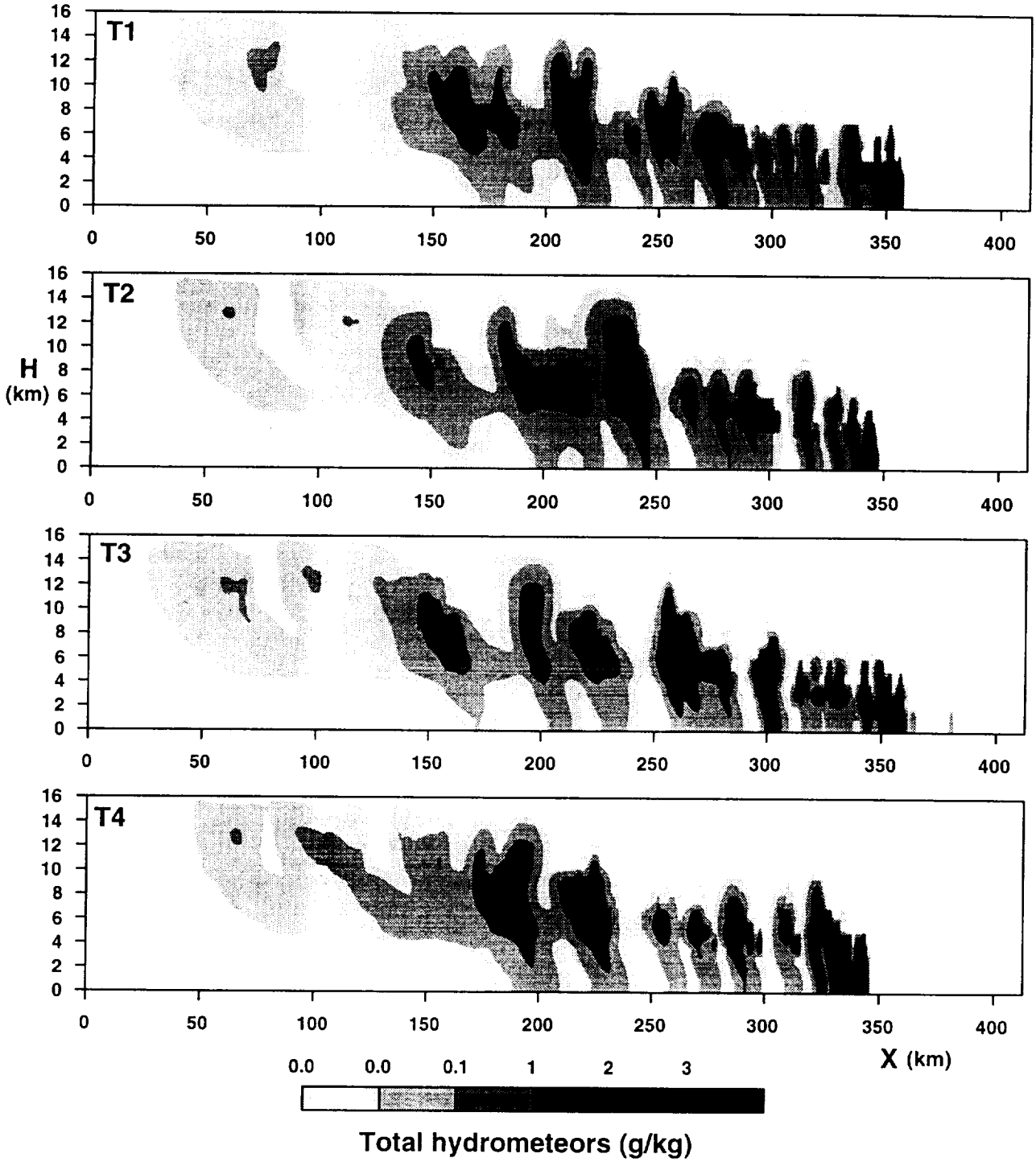
T1
T2
T3
T4
H (km)
X (km)
0 50 100 150 200 250 300 350 400
0 2 4 6 8 10 12 14 16
0.0 0.0 0.1 1 2 3
Total hydrometeors (g/kg)

Fig. 4

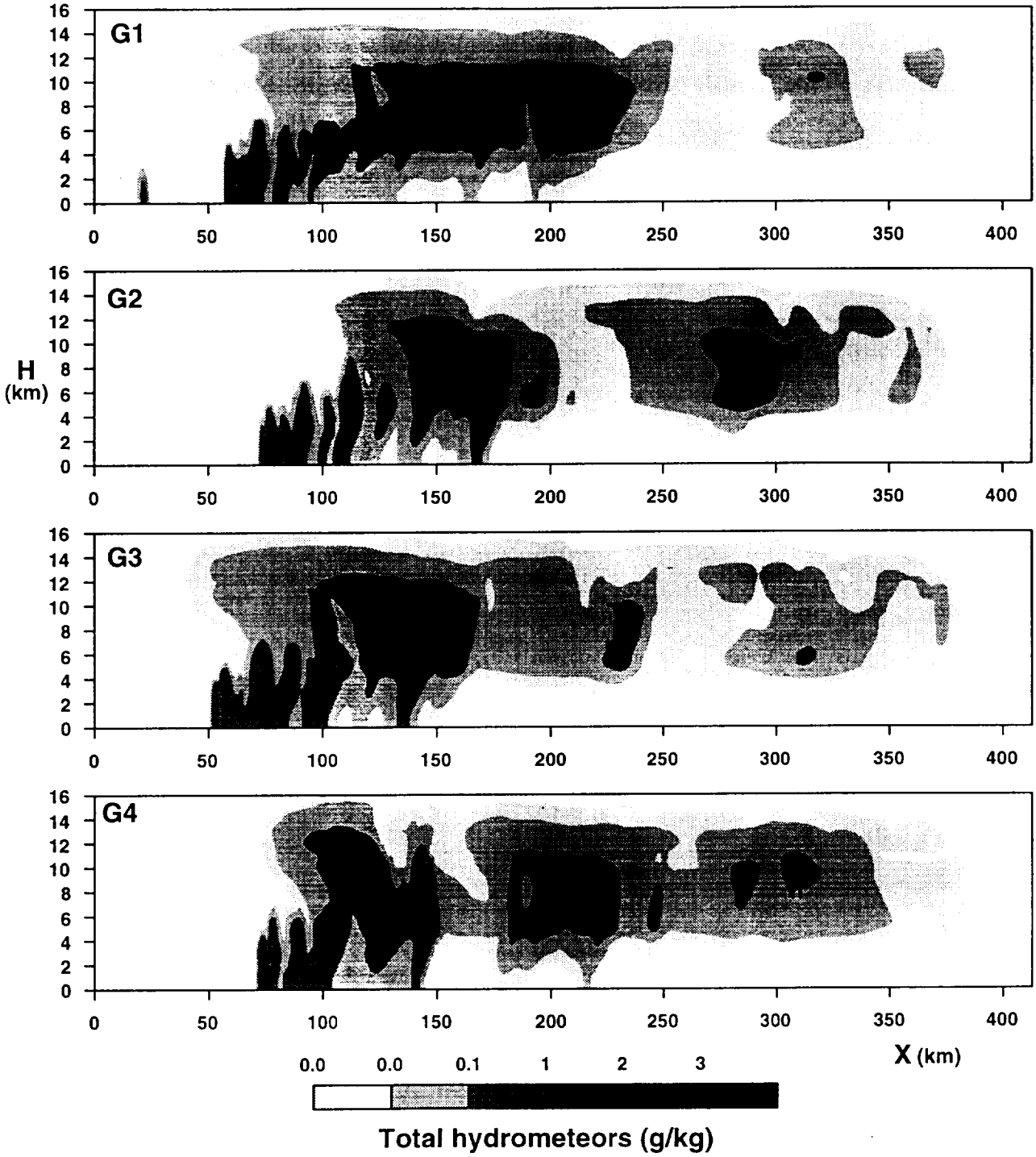
G1
G2
G3
G4
H
(km)
0
2
4
6
8
10
12
14
16
0
50
100
150
200
250
300
350
400
X (km)
0.0
0.0
0.1
1
2
3
Total hydrometeors (g/kg)

Fig. 5

Fig. 6

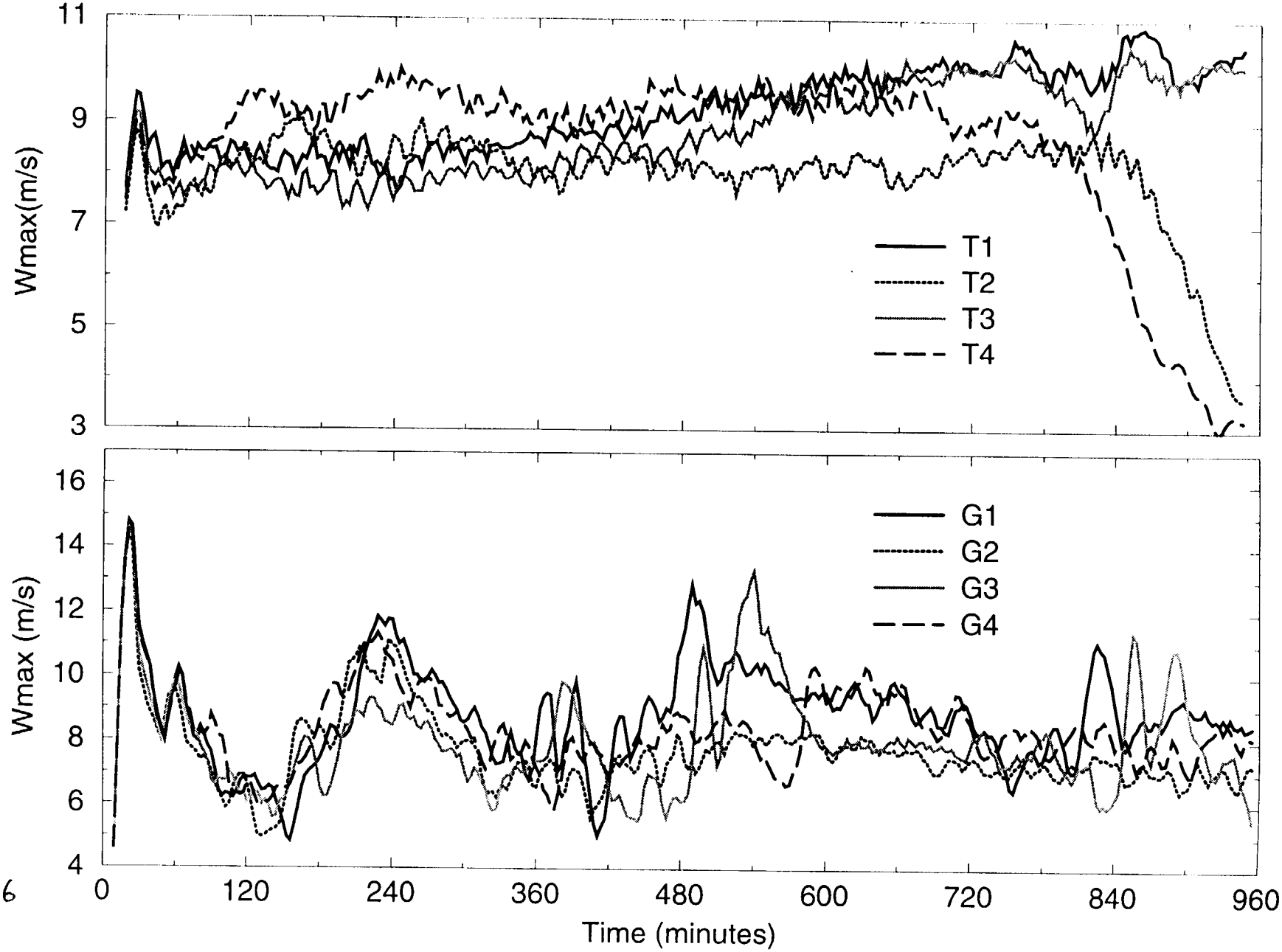
Wmax(m/s)
11
9
7
5
3
T1
T2
T3
T4
Wmax (m/s)
16
14
12
10
8
6
4
G1
G2
G3
G4
0
120
240
360
480
600
720
840
960
Time (minutes)

Fig. 6

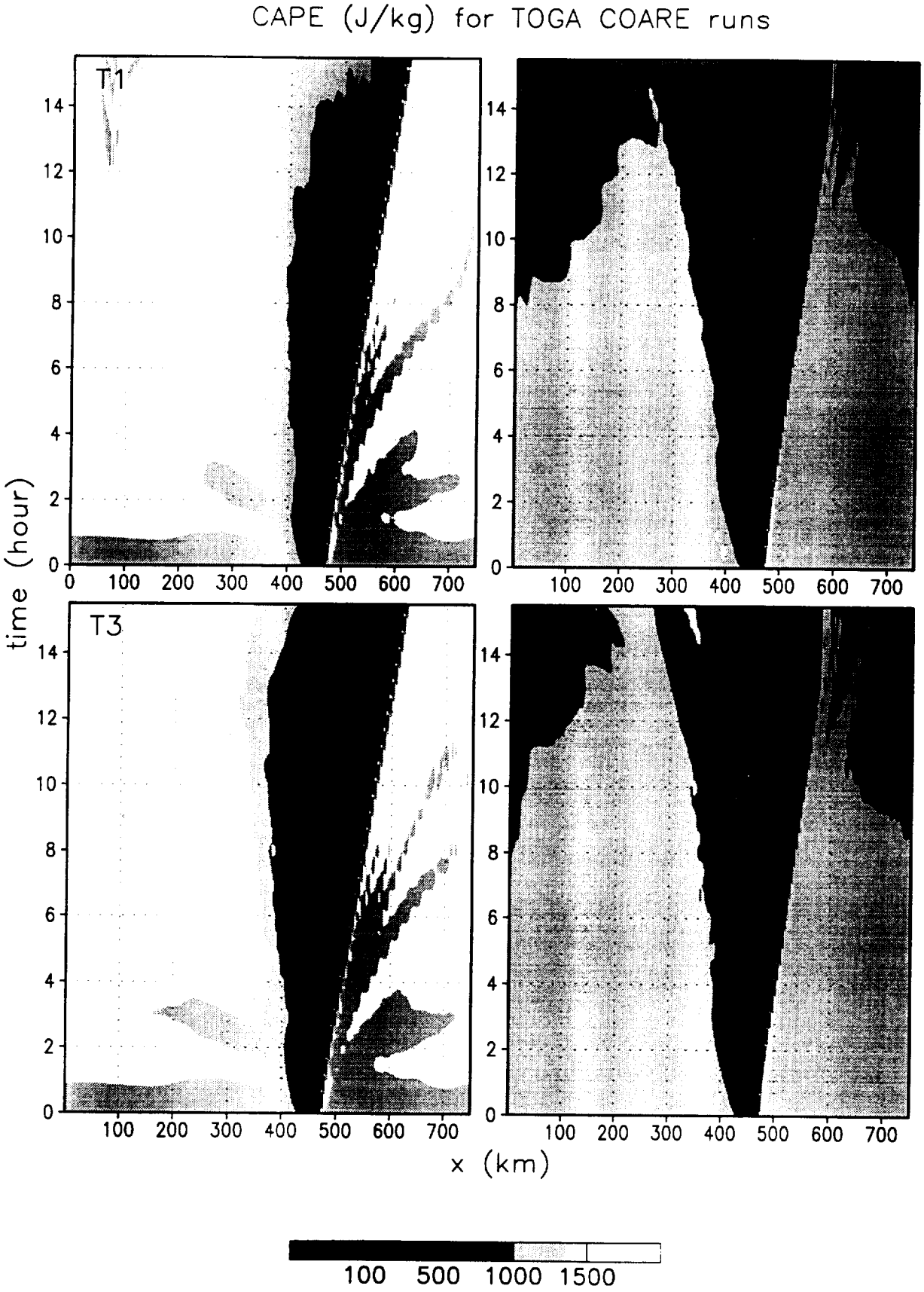
CAPE (J/kg) for TOGA COARE runs
T1
T3
time (hour)
x (km)
0
2
4
6
8
10
12
14
100
200
300
400
500
600
700
100
500
1000
1500

Fig. 7

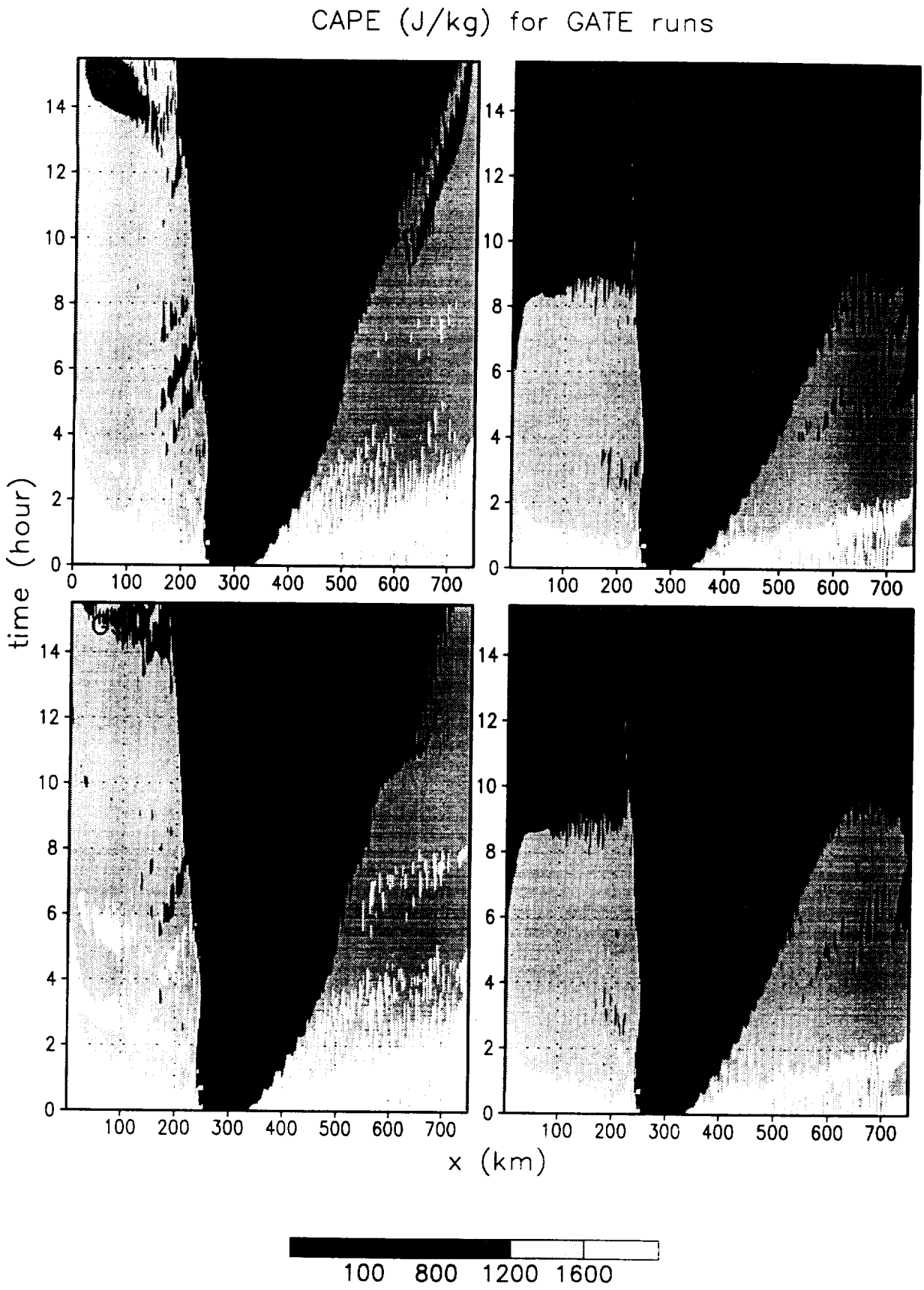
CAPE (J/kg) for GATE runs
time (hour)
x (km)
0
2
4
6
8
10
12
14
100
200
300
400
500
600
700
100
800
1200
1600

Fig. 8

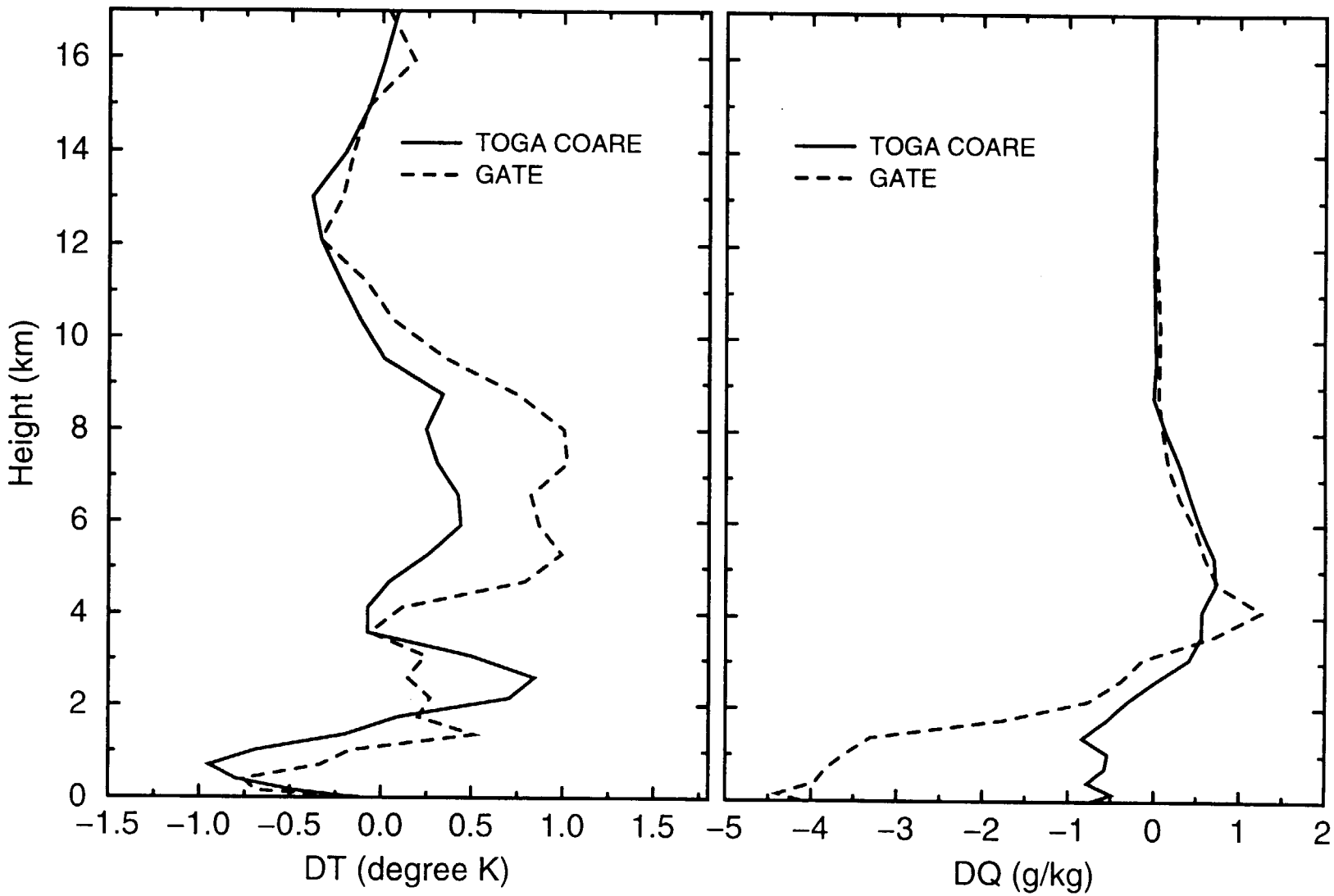
Height (km)
16
14
12
10
8
6
4
2
0
TOGA COARE
GATE
−1.5 −1.0 −0.5 0.0 0.5 1.0 1.5
DT (degree K)
TOGA COARE
GATE
−5 −4 −3 −2 −1 0 1 2
DQ (g/kg)

Fig. 9

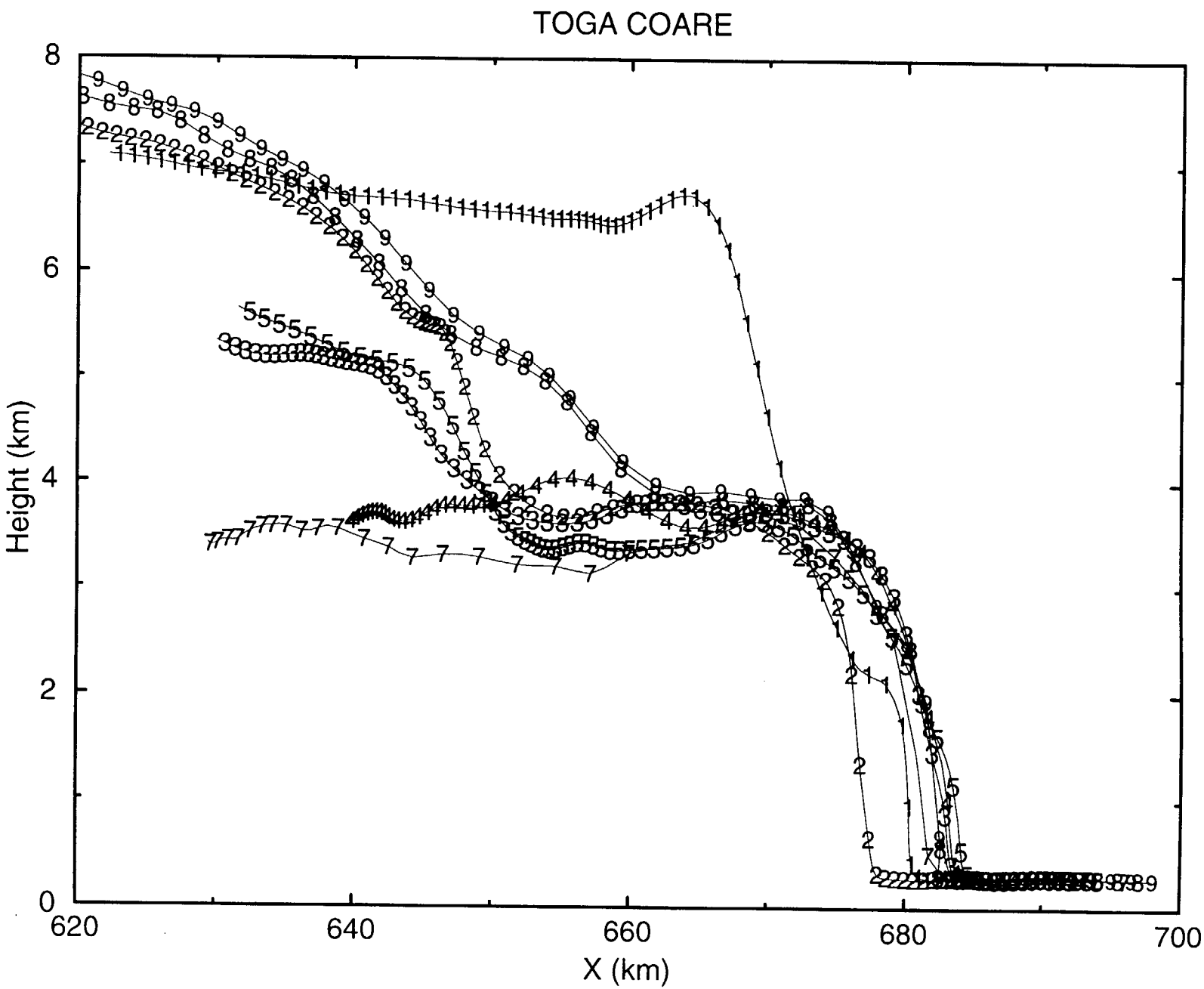

Fig 10

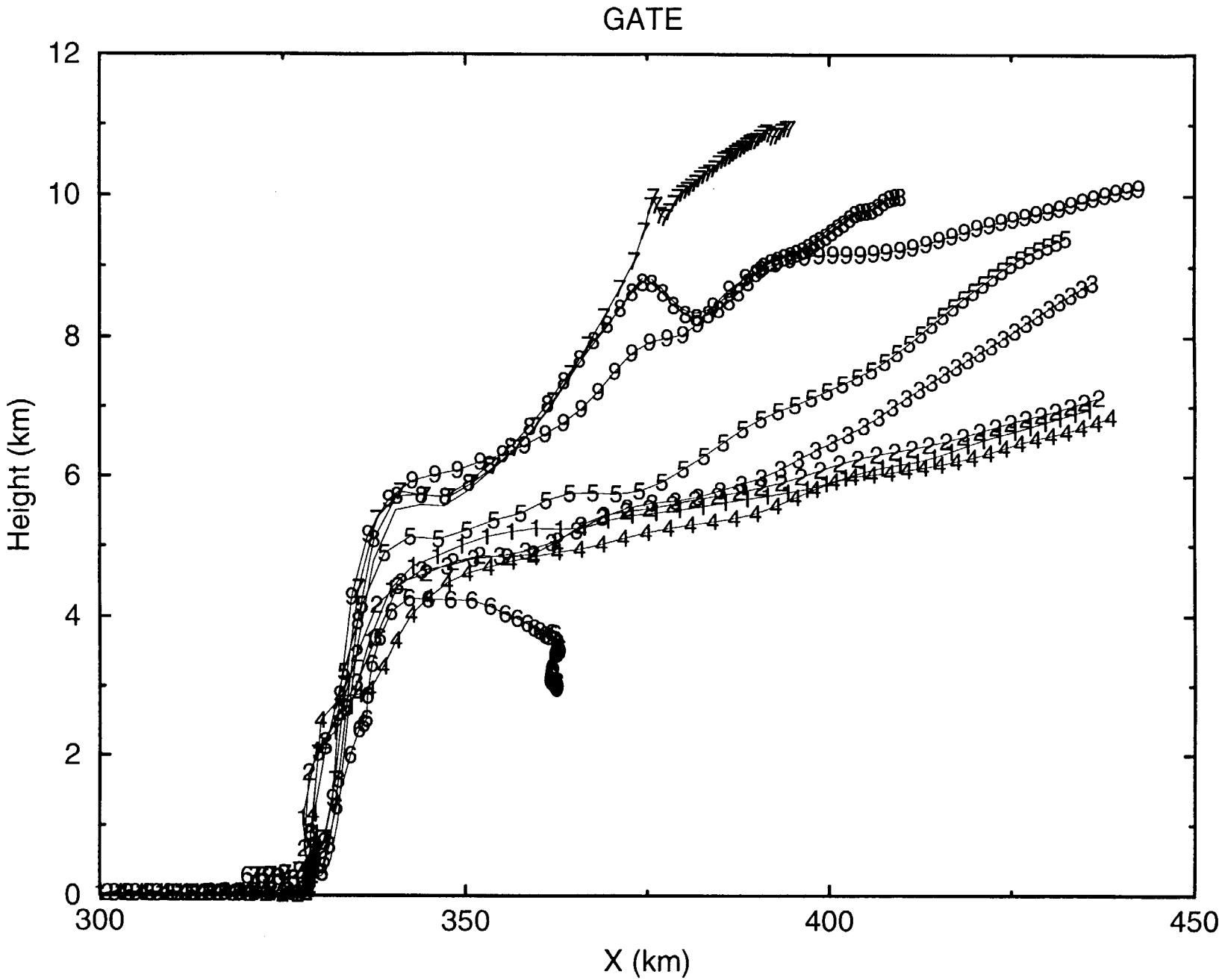

Fig. 11

schematic diagram shown water budget computation

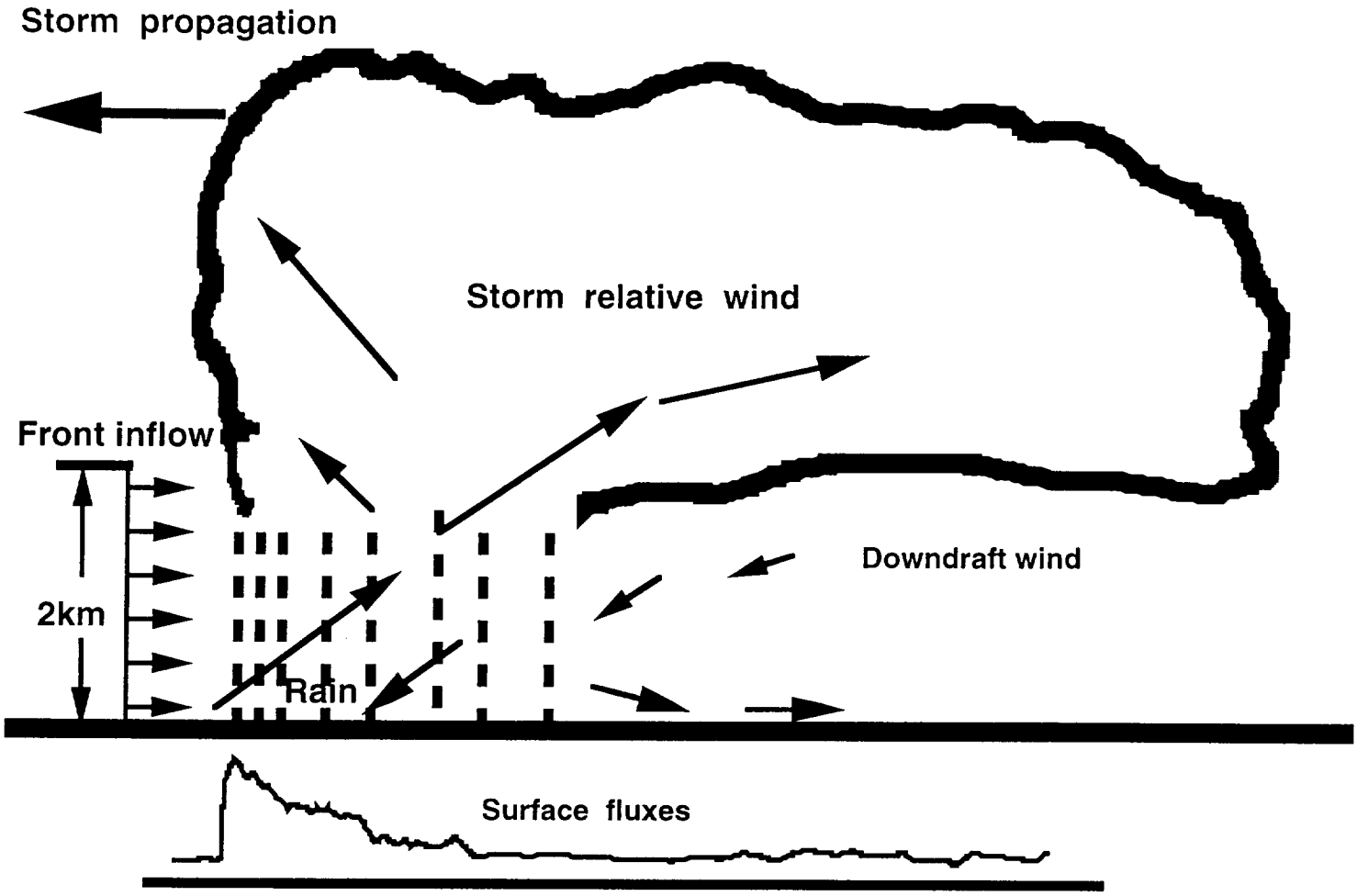

Fig. 12